

Abstract

Greenland ice sheet mass loss has accelerated in the past decade responding to combined glacier discharge and surface melt water runoff increases. During summer, absorbed solar energy, modulated at the surface primarily by albedo, is the dominant factor governing surface melt variability in the ablation area. Using satellite observations of albedo and melt extent with calibrated regional climate model output, we determine the spatial dependence and quantitative impact of the ice sheet albedo feedback in twelve summer periods beginning in 2000. We find that while the albedo feedback is negative over 70 % of the ice sheet, concentrated in the accumulation area above 1500 m, positive feedback prevailing over the ablation area accounts for more than half of the overall increase in melting. Over the ablation area, year 2010 and 2011 absorbed solar energy was more than twice as large as in years 2000–2004. Anomalous anticyclonic circulation, associated with a persistent summer North Atlantic Oscillation extreme since 2007 enabled three amplifying mechanisms to maximize the albedo feedback: (1) increased warm (south) air advection along the western ice sheet increased surface sensible heating that in turn enhanced snow grain metamorphic rates, further reducing albedo; (2) increased surface downward solar irradiance, leading to more surface heating and further albedo reduction; and (3) reduced snowfall rates sustained low albedo, maximizing surface solar heating, progressively lowering albedo over multiple years. The summer net radiation for the high elevation accumulation area approached positive values during this period.

1 Introduction

Greenland ice sheet mass balance fluctuations exert an important influence on global sea level while changes to its cryosphere provide useful indicators of climate change. Between 1961 and 1990, a period in which the Greenland ice sheet was in relative balance (Rignot et al., 2008), the annual accumulation totaled $\sim 700 \text{ Gt yr}^{-1}$, balanced

TCD

6, 593–634, 2012

Greenland ice sheet albedo feedback

J. E. Box et al.

Title Page

Abstract

Introduction

Conclusions

References

Tables

Figures

◀

▶

◀

▶

Back

Close

Full Screen / Esc

Printer-friendly Version

Interactive Discussion



**Greenland ice sheet
albedo feedback**

J. E. Box et al.

Title Page

Abstract

Introduction

Conclusions

References

Tables

Figures

◀

▶

◀

▶

Back

Close

Full Screen / Esc

Printer-friendly Version

Interactive Discussion



by $\sim 480 \text{ Gt yr}^{-1}$ glacier discharge and $\sim 220 \text{ Gt yr}^{-1}$ runoff losses (Ettema et al., 2009). Subsequently, satellite gravimetry reveals overall mass loss (Chen et al., 2011) due to a combination of increased surface melting (Mote, 2007; Fettweis et al., 2011a) and runoff (Box et al., 2006; Ettema et al., 2009), peripheral dynamic thinning (Krabill et al., 2004; Pritchard et al., 2009) and increased glacier discharge (Rignot et al., 2006; Howat et al., 2008). During summer, absorbed solar energy, modulated at the surface primarily by albedo, is the dominant factor governing surface melt variability in the ablation area (van den Broeke et al., 2008). The current mass loss appears to be dominated by either ice discharge or surface ablation depending on which mass flux is greatest in a given year (Rignot et al., 2006; van den Broeke et al., 2009).

Changes in snow and ice cover duration and area have an amplifying effect on climate in warming and cooling scenarios from the self-reinforcing surface albedo feedback with temperature. Hall (2004) reviews numerous relevant publications. Warming reduces albedo even without removing snow or ice cover, through the increase of snow grain size from snow crystal metamorphism (Wiscombe and Warren, 1980; Dozier et al., 2009; Warren, 1982). The feedback operates in reverse with cooling associated with higher albedo from more persistent snow cover, lower rain to snowfall ratios, and less positive surface radiation budget.

An assessment of northern hemispheric satellite and regional climate model data (Flanner et al., 2011) derives top of the atmosphere ice-albedo feedback magnitudes between 0.3 and $1.1 \text{ W m}^{-2} \text{ K}^{-1}$. Fernandes et al. (2009) measured surface albedo sensitivity to surface air temperature (T_{air}) for land surfaces poleward of 30° N to be $-0.93 \pm 0.06 \text{ \% K}^{-1}$ with maximum albedo sensitivity exceeding -9 \% K^{-1} over the northern terrestrial environments where the albedo difference between snow cover and bare land reaches maximum values up to ~ 0.7 . This study did not analyze albedo sensitivity for the Greenland ice sheet, presumably because downscaling would have been necessary to resolve the ice sheet ablation area.

Stroeve (2001) assessed Greenland ice sheet albedo variability using monthly averaged albedo from the AVHRR Polar Pathfinder (APP) data set spanning 1981–1998.

Greenland ice sheet albedo feedback

J. E. Box et al.

Title Page

Abstract

Introduction

Conclusions

References

Tables

Figures

◀

▶

◀

▶

Back

Close

Full Screen / Esc

Printer-friendly Version

Interactive Discussion



The study found: 1) anomalously low albedo during the warm years of 1995 and 1998; 2) high albedo in 1992, associated with the low temperature anomaly caused by the Mt. Pinatubo eruption (Abdalati and Steffen, 2001); 3) correspondence of the remotely sensed albedo with in-situ observations from Greenland Climate Network (GC-Net) automatic weather stations (AWS) (Steffen et al., 1996); 4) correlation between changes in albedo with the NAO index; and 5) an overall negative albedo trend over the 1981–1998 period of study. Box et al. (2006) found a decline in ice sheet albedo for the 2000–2004 period using Moderate-Resolution Imaging Spectroradiometer (MODIS) data.

The primary objective of this study is to quantify the spatial patterns of ice sheet albedo change and the ice-albedo feedback for the Greenland ice sheet. This is accomplished using satellite observations and regional climate model output calibrated with in-situ observations. The surface energy budget is examined to identify key melt sensitivities. Analysis of regional atmospheric circulation anomalies permits attribution of the triggers and key mechanisms of the albedo feedback.

2 Data

2.1 In-situ observations

GC-Net AWS (Steffen et al., 1996) provide hourly averages of 15 s measurements of surface upward and downward solar irradiance ($S \downarrow$ and $S \uparrow$, respectively). The LI-COR 200 SZ pyranometers are sensitive in the 0.4 to 1.1 μm wavelength range. A +0.035 bias offset in 200 SZ albedo was derived by Stroeve et al. (2006) in comparison with broadband (0.3 to 3.0 μm) pyranometers observations, owing to incomplete broadband sensitivity of the downward facing LI-COR pyranometer. $S \downarrow$ was found to be accurately measured. T_{air} is sampled at 15 s intervals using thermocouples and at 60 s using Vaisala HMP45C thermistors shielded from direct solar irradiance by naturally-aspirated white plastic enclosures. A 2–3 K root mean squared error (RMSE) correspondence is found between the hourly T_{air} observations and satellite clear-sky

MODIS surface temperature retrievals over Greenland (Hall et al., 2008). In this study, the GC-Net T_{air} data are quality controlled by rejecting hourly data for which there is a disagreement > 0.5 K between the redundant sensor types before computing monthly averages. At least 90 % of possible cases must be available for monthly averages to be calculated and used in this study. Albedo computed from GC-Net $S \downarrow$ and $S \uparrow$ data is quality controlled on a monthly basis by rejecting albedo associated with monthly total $S \uparrow$ exceeding $S \downarrow$. Other cases of obvious pyranometer failure are rejected, for example due to heavy rime frost accretion when calculated monthly albedo values differ in the absolute by more than 0.2 from the satellite data.

2.2 Satellite-derived albedo

Daily surface albedo retrievals from the NASA Terra platform MODIS sensor MOD10A1 product beginning day 65 in 2000 are available from the National Snow and Ice Data Center (NSIDC) (Hall et al., 2011). Release version 005 data are compiled over Greenland spanning March 2000 to October 2011. Surface albedo is calculated using the first seven visible and near-infrared MODIS bands (Klein and Stroeve, 2002; Klein and Barnett, 2003). The MOD10A1 product contains snow extent, snow albedo, fractional snow cover, and quality assessment data at 500 m resolution, gridded in a sinusoidal map projection. To reduce computational burdens, the data are resampled using a nearest-neighbor approach to 5 km using the Equal Area Scalable Earth (EASE) grid using NSIDC re-gridding utilities (<http://nsidc.org/data/modis/ms2gt/>). The 5 km spatial resolution permits resolving the ablation area within the goals of this study. Major gaps in the time series occur in year 2000, days 211–231 and year 2001, days 165–188. The frequency and quality of spaceborne albedo retrievals decreases substantially in non-summer months as the amount of solar irradiance and its incidence angle decreases. Also, in non-melting periods before April and after September, there are few valid data, especially in Northern Greenland because of the extremely low solar incidence. The accuracy of retrieving albedo from satellite or ground-based instruments declines as the solar zenith angle (SZA) increases, especially beyond $\sim 75^\circ$, resulting

Greenland ice sheet albedo feedback

J. E. Box et al.

Title Page

Abstract

Introduction

Conclusions

References

Tables

Figures

◀

▶

◀

▶

Back

Close

Full Screen / Esc

Printer-friendly Version

Interactive Discussion



in many instances of albedo values that exceed the expected maximum clear sky snow albedo of 0.84 (Konzelmann and Ohmura, 1995). Here, we limit these data by focusing on the June–August period when SZA is minimized when the albedo retrievals are made.

Stroeve et al. (2006) concluded that the MOD10A1 data product captured the natural seasonal cycle in albedo, but exhibited significantly more temporal variability than recorded by ground observations. We now understand that a dominant component of this assessed error is the failure of the MODIS data product to completely remove cloud effects. Inspection of the raw MOD10A1 images reveal an abundance of residual cloud artifacts (shadows, contrails, thin clouds, cloud edges) in the albedo product, presumably because the similar spectral properties between snow and some clouds results in obvious cloud structures. Another problem consists of spuriously low values, for example below 0.4 in the accumulation area where albedo is not observed by pyranometers at the surface to drop below 0.7, seen as linear stripe artifacts in the imagery. Because both the cloud shadows and stripes introduce abrupt daily departures from the actual albedo time series, it is possible to reject them using a multi-day sample. Thus, on a pixel-by-pixel basis, 11-day running statistics are used to identify and reject values that exceed 2 standard deviations (2σ) from an 11-day average. To prevent rejecting potentially valid cases data within 0.04 of the median are never rejected. The 11-day median is taken to represent each pixel in the daily data and has a smoothing effect on the albedo time series. June–August (JJA or summer) seasonal averages are generated from monthly averages of the daily filtered (and smoothed) data. For simplicity, data from the MODIS Aqua instrument are not used in this study.

2.3 MODIS MOD10A1 validation

We compare MOD10A1 albedo with GC-Net albedo for the 2000–2010 time period at 17 GC-Net sites within the 550–3250 m elevation range. Months with less than 90% possible of the hourly samples data are not considered. Under high SZA, GC-Net LI-COR 200-SZ pyranometer errors become extreme, especially for the

Greenland ice sheet albedo feedback

J. E. Box et al.

Title Page

Abstract

Introduction

Conclusions

References

Tables

Figures

◀

▶

◀

▶

Back

Close

Full Screen / Esc

Printer-friendly Version

Interactive Discussion



downward facing sensor. This “cosine response” error is minimized by using monthly totals of hourly data in the albedo calculation:

$$\alpha = \frac{\sum S \uparrow}{\sum S \downarrow} \quad (1)$$

While cases when SZA is high are included in this calculation their contribution to the total is negligible (van den Broeke et al., 2004). Averaging MODIS data within 10 km of the GC-Net AWS location yields RMSE values of 0.041 ± 0.011 (Fig. 1). This RMSE finding is smaller by nearly a factor of two than earlier found because monthly instead of daily means are considered and the outlier rejection described in the previous section greatly reduces spurious temporal variability. While the residual bias (-0.006 ± 0.008) is indistinguishable from zero, there is evidence of positive skew in the MODIS data above 0.84 when pyranometers report albedo exceeding 0.84 only under cloudy skies. Ground measurements of albedo greater than 0.84 under cloudy conditions is attributable to the relative increase in the absorption of the downward near infrared solar irradiance by clouds. The MODIS albedo algorithm on the other hand does not provide a surface albedo estimate under cloudy skies. In addition, extremely high (> 0.9) MOD10A1 values are found at high elevations in the most northerly latitudes where SZA is high, and when the uncertainty in the MOD10A1 albedo is also high as noted by the accompanying data quality flag. It is nonetheless possible to conclude that the MOD10A1 product is accurate in representing Greenland ice sheet albedo in the range from 0.26 to 0.84 in which we have nearly simultaneous and coincident GC-Net AWS observations. An ice sheet mask is used to verify that minimum ice sheet albedo values in the MOD10A1 product are 0.31. The lowest reported GC-Net albedo measurement (0.259) is from the JAR1 site for July 2010. The JAR1 AWS is situated in the most impurity rich parts of the ablation area (Wientjes and Oerlemans, 2010) where values of 0.31 are estimated by (Knapp and Oerlemans, 1996).

Greenland ice sheet albedo feedback

J. E. Box et al.

Title Page

Abstract

Introduction

Conclusions

References

Tables

Figures

◀

▶

◀

▶

Back

Close

Full Screen / Esc

Printer-friendly Version

Interactive Discussion



2.4 The MAR regional climate model

The observationally-constrained Modèle Atmosphérique Régional (MAR) (Fettweis et al., 2011a) is coupled with a one-dimensional multi-layered energy balance snow model (Gallée and Schayes, 1994; Lefebre et al., 2003). The temperature, albedo, precipitation and surface melt simulated by MAR have been validated (Lefebre et al., 2003, 2005; Fettweis et al., 2005, 2011a,b). The ability of MAR to realistically simulate the surface mass balance over the ice sheet has been established (Fettweis, 2007; Tedesco et al., 2011). The MAR version used here is calibrated to best compare with the satellite passive microwave derived melt extent from 1979–2009 (Fettweis et al., 2011a). A tundra/ice mask is used based on the Greenland land surface classification mask from a MODIS classification (http://bprc.osu.edu/wiki/Jason_Box_Datasets) and the model terrain (Bamber et al., 2001) is smoothed (Fettweis et al., 2005). MAR is run with a horizontal resolution of 25 km and is forced each 6 h at the lateral boundaries by the European Centre for Medium Range Weather Forecasts (ECMWF) ERA-INTERIM reanalysis (Dee et al., 2011). MAR data are attractive for use here because they are available at higher spatial resolution than global re-analyses, just sufficient to resolve spatial gradients in T_{air} and $S \downarrow$. Here, the MAR data are resampled and reprojected to the 5 km MODIS albedo data grid (EASE-Grid), described earlier.

2.5 MAR validation

GC-Net data are used to evaluate the accuracy of MAR simulations of $S \downarrow$ and T_{air} . At monthly time scales, for $S \downarrow$, we find that the MAR RMSE is equivalent to the GC-Net sensor uncertainty of 15 W m^{-2} , equal to the 5 % instrument specifications under 300 W m^{-2} irradiance. The average biases are less than the specified GC-Net sensor error. However, a systematic bias is evident for June, July, and August, with regression slopes between 0.81 and 0.84, suggesting that MAR has 16–19 % too much shortwave cloud opacity in the lower half of the distribution. To meet the goal of assessing the albedo feedback with absolute accuracy, the regression functions illustrated in Fig. 2

TCO

6, 593–634, 2012

Greenland ice sheet albedo feedback

J. E. Box et al.

Title Page

Abstract

Introduction

Conclusions

References

Tables

Figures

◀

▶

◀

▶

Back

Close

Full Screen / Esc

Printer-friendly Version

Interactive Discussion



are used to calibrate MAR $S \downarrow$. Only JJA data are used in this study to evaluate the albedo feedback. Assuming all absolute and systematic error is attributed to MAR and that these errors are temporally homogeneous, the monthly regression functions are applied to the monthly average MAR data prior to calculating seasonal averages.

Monthly averages from GC-Net for the 2000–2010 period are used to evaluate the accuracy of monthly average MAR simulations of T_{air} illustrated in Fig. 3. The average bias grows from 0°C in June with an RMSE of 1.1°C to a minor positive bias in July and an obvious systematic bias in August. The MAR cold bias in July/August is a consequence of an underestimation of $L \downarrow$ (Fettweis et al., 2011a). However, it should be noted that this bias occurs for pixels with temperatures below -10°C where little melting is simulated. As with $S \downarrow$, to minimize bias, the MAR T_{air} data are calibrated using the monthly regression functions. The post-calibration RMSE is 1.0°C .

Additional MAR variables used in this study include the turbulent heat fluxes: Q_{SH} and Q_{LH} . Energy fluxes that heat the surface are positive in this budget. The net turbulent flux ($Q_{\text{SH}} + Q_{\text{LH}}$) is also referred to in this study. Downward longwave irradiance ($L \downarrow$) is used to evaluate changes in all-sky downward thermal emission. Similarly, the total downward irradiance, the sum of $S \downarrow + L \downarrow$, hereafter $R \downarrow$ is useful to evaluate total surface incident radiation flux density.

2.6 Surface mass balance

Grey tones in Fig. 4 indicate the mean ablation area over the 2000–2011 period, according to MAR, where the calculated annual melt and runoff exceed the snow accumulation rate and the surface mass balance (SMB) is negative. Colored regions indicate the accumulation area according to MAR where SMB is positive. The *equilibrium line* separates the $\sim 1.428 \pm 0.131 \times 10^6 \text{ km}^2$ net snow *accumulation area* from the $0.414 \pm 0.249 \times 10^6 \text{ km}^2$ net ice *ablation area*. The km^2 areas are from the MAR simulations in the 2000–2011 period. The values following “ \pm ” indicate 1σ of 11 hydrologic year samples ending in 2011.

Greenland ice sheet albedo feedback

J. E. Box et al.

Title Page

Abstract

Introduction

Conclusions

References

Tables

Figures

I◀

▶I

◀

▶

Back

Close

Full Screen / Esc

Printer-friendly Version

Interactive Discussion



2.7 Surface melt extent

Greenland melt extent is mapped using passive microwave observations from the NOAA/NASA Pathfinder SSM/I Level 3 EASE-Grid Brightness Temperature data recorded by the Special Sensor Microwave/Imager (SSM/I) flown on the satellites of the Defense Meteorological Satellite Program (DMSP, F08, F11, F13 and F17). The data are gridded to a 25 km resolution (http://nsidc.org/data/docs/daac/nsidc0032_ssmi_ease_tbs.gd.html) and are available from NSIDC (<http://nsidc.org/data/nsidc-0032.html>). When snow melts, the imaginary part of snow permittivity increases as a consequence of the presence of liquid water, causing an increase in the absorption and, therefore, microwave brightness temperature (Chang et al., 1976; Mote and Anderson, 1995; Abdalati and Steffen, 2001; Mote, 2007; Tedesco, 2007; Fettweis et al., 2011a). Conversely, brightness temperatures over dry snow are relatively low and this is especially true in Greenland where ice (not land) lies below the snowpack. Brightness temperatures can also increase because of a decrease in effective grain size due to new snow or changes in snow temperature. However, these processes are much slower than those associated with the appearance of liquid water within the snowpack within a diurnal cycle. Melting is here detected when the difference between ascending and descending brightness temperatures (DAV) measured at 19.35 GHz, or when the absolute value of either ascending or descending brightness temperatures exceed the estimated threshold values (Tedesco, 2007).

3 Methods

The physical processes driving surface melt over ice are isolated using a surface energy budget (SEB):

$$SEB = Q_{SH} + Q_{LH} + Q_G + L_{net} + S_{net} \quad (2)$$

TCD

6, 593–634, 2012

Greenland ice sheet albedo feedback

J. E. Box et al.

Title Page

Abstract

Introduction

Conclusions

References

Tables

Figures

◀

▶

◀

▶

Back

Close

Full Screen / Esc

Printer-friendly Version

Interactive Discussion



where Q_{SH} and Q_{LH} are the turbulent sensible and latent heat fluxes, respectively. Persistent temperature inversions over ice sheets lead Q_{SH} to be an energy source most of the year (van den Broeke et al., 2008). Q_{LH} is an energy sink where evaporation or sublimation absorb latent heat. Q_{LH} can be a melt energy source in the lower ablation area (van den Broeke et al., 2008). Q_G is the subsurface conductive sensible heat flux. L_{net} is the difference between downward and upward infrared irradiance ($L \downarrow - L \uparrow$). S_{net} represents surface absorbed solar energy, depends on $S \downarrow$ and the surface albedo (α) defined as the ratio of the upward to downward solar irradiance in the 0.3 μm to 4 μm spectrum:

$$S_{net} = S \downarrow (1 - \alpha) \quad (3)$$

$S \downarrow$ peaks in summer months and is modulated by cloud optical thickness and solar illumination geometry which depends significantly on the 23° latitudinal extent of the ice sheet. Units of energy fluxes are (W m^{-2}).

Melt water volume (M) expressed in units of mm water equivalence (mm w.e.) is calculated by MAR from surface energy budget closure:

$$M = (R_N - (Q_{SH} + Q_{LH} + Q_G)\Delta t)(L_f \rho)^{-1} \quad (4)$$

where Δt is the time interval (s); L_f is the latent heat of fusion ($3.335 \times 10^5 \text{ J kg}^{-1}$); and ρ is the density of water (1000 kg m^{-3}). The associated melt extent has been validated (Tedesco et al., 2011) with SMB observations from the K-transect along the western ice sheet and with satellite microwave observations (Fettweis et al., 2011a). The inter-annual variability and magnitude of MAR-derived M , driven by the ERA-Interim reanalysis, correspond closely with the in situ and satellite-derived observations. As for the unvalidated parameters Q_{SH} and Q_{LH} , it is the relative and inter-annual magnitude of variability rather than the absolute magnitude that is of primary interest. MAR-simulated Q_G for June–August is found to be the smallest SEB term, approaching zero in the upper m of the ablation area and is not analyzed further in this study.

Greenland ice sheet albedo feedback

J. E. Box et al.

Title Page

Abstract

Introduction

Conclusions

References

Tables

Figures

◀

▶

◀

▶

Back

Close

Full Screen / Esc

Printer-friendly Version

Interactive Discussion



Passive microwave-derived melt extent (Tedesco, 2007) permits defining surface melt duration (Δt) such that melt volume attributable to S_{net} may be partitioned from melt volume attributable to other SEB terms.

The albedo sensitivity to near-surface air temperature (at ~ 3 m above the surface in MAR calculations), expressed here in units of % albedo K^{-1} is determined by regression between 12 annual samples of detrended anomalies of June–August average α and T_{air} . Similarly, we quantify the albedo feedback in units of $\text{W m}^{-2} \text{K}^{-1}$ using summer average α , S_{net} and T_{air} :

$$\alpha_{\text{Feedback}} = \Delta S \downarrow (1 - \Delta\alpha) / \Delta T_{\text{air}} = \Delta S_{\text{net}} / \Delta T_{\text{air}} \quad (5)$$

Freshly fallen snow under clear skies has an albedo of ~ 0.84 (Konzelmann and Ohmura, 1995), progressively reducing during the sunlit (warm) season as a consequence of ice grain growth, resulting in a self-amplifying albedo decrease. The complete melting of the winter snow accumulation on ice sheets at the low elevations exposes underlying glacier ice in the ablation area. In this region, the albedo of low-impurity snow-free glacier ice is in the range of 0.30 to 0.60 (Cuffey and Paterson, 2010). Where aeolian and microbiological impurities accumulate near the glacier ice surface (Bøggild et al., 2010), the albedo may be extremely low (0.20) (Cuffey and Paterson, 2010). Thus, intraseasonal summer albedo variability exceeds 0.50 over parts of the ice sheet where a snow layer ablates by mid-summer, exposing an impurity-rich ice surface (Knap and Oerlemans, 1996; Wientjes and Oerlemans, 2010), resulting in S_{net} being the largest source of energy for melting during summer and explaining most of the inter-annual variability in melt totals (van den Broeke et al., 2011).

The accumulation area is also susceptible to albedo feedback from grain growth metamorphism occurring in sub-freezing conditions. Temporal changes in any of the variables are considered “significant” if the 12-yr regression slope multiplied by the number of years, i.e., the “change”, exceeds 1σ of the residuals of the linear fit. The 1σ uncertainty envelope is presented immediately after slope values using the \pm symbol.

Greenland ice sheet albedo feedback

J. E. Box et al.

Title Page

Abstract

Introduction

Conclusions

References

Tables

Figures

◀

▶

◀

▶

Back

Close

Full Screen / Esc

Printer-friendly Version

Interactive Discussion



4 Results

4.1 Albedo seasonal and inter-annual variability

The average albedo of the ice sheet declines from 0.835 in April to 0.707 by mid July (Fig. 5). Meltwater production and extent according to spaceborne passive microwave remote sensing data generally peak in July (Mote, 2007), when T_{air} reaches its annual maximum. As the melt season ends, snow accumulation brightens the surface. Yet, because of extreme 2010 melt and little snow accumulation during the melt season (Tedesco et al., 2011) and afterward, the ice sheet albedo remained more than 2σ below the 2000–2011 average in October. In the following year, June and July 2011 ice sheet albedo reached its lowest observed values despite temperatures being on average lower than in 2010, suggesting a progressive multi-year albedo decline from albedo feedback.

According to linear regression, the ablation area albedo declined from 0.715 in 2000 to 0.632 in 2011 (time correlation = -0.805 , $1 - p = 0.999$). The change (-0.083) is more than two times the absolute albedo RMSE (± 0.041). Over the accumulation area, the highly linear (time correlation = -0.927 , $1 - p > 0.999$) decline from 0.817 to 0.766 over the same period also exceeds the absolute albedo RMSE.

4.2 Albedo trend verification

Degrading MODIS instrument sensitivity identified by Wang et al. (2012) introduces the possibility that the declining albedo trends may be erroneous. To validate the MODIS albedo trends, coinciding observations from GC-Net AWS are examined. The ground truth data are situated across a range of elevations, spanning the ablation and accumulation areas.

Analysis of the GC-Net data confirm declining albedo trends in the 2000–2010 period to be widespread in individual months from May–September. Trend statistics are computed where at least 7 yr of annual data are available from both GC-Net and MODIS

Greenland ice sheet albedo feedback

J. E. Box et al.

Title Page

Abstract

Introduction

Conclusions

References

Tables

Figures

◀

▶

◀

▶

Back

Close

Full Screen / Esc

Printer-friendly Version

Interactive Discussion



**Greenland ice sheet
albedo feedback**

J. E. Box et al.

Title Page

Abstract

Introduction

Conclusions

References

Tables

Figures

◀

▶

◀

▶

Back

Close

Full Screen / Esc

Printer-friendly Version

Interactive Discussion



Terra. Significance is designated where the trend measured by the linear regression slope has a magnitude that exceeds 2σ of the residuals from the regression. In 41 of 43 (95 %) of monthly cases May–September, the trend is found to be significant and decreasing (Table 1). In 10 of 14 (71 %) cases for which both GC-Net and MOD10A1 trends are significant, the GC-Net trend declining trend is larger than the MOD10A1 trend. It therefore does not seem that MODIS sensor degradation is enhancing an existing trend.

It seems improbable that degradation of the GC-Net photoelectric diode pyranometers are producing an erroneous declining albedo trend. If both upward and downward facing sensors degrade at the same rate, the albedo would not change in time due to progressive sensor bias. An erroneous declining trend would require that the downward facing pyranometer degrade faster than the upward facing pyranometer. If the degradation is increased by exposure to sunlight as it is with optical optical black lacquer pyranometers, then the upward pyranometer would be expected degrade faster, introducing an erroneous *increasing* albedo trend. We observe the opposite.

The largest magnitude declining albedo trends are evident at the sites located in the ablation zone such as JAR1 and Swiss Camp. The more southerly yet relatively high elevation sites of Saddle and South Dome where melting is uncommon in passive microwave observations (e.g., Mote, 2007; Tedesco, 2007), declining albedo trends are observed consistently in individual months (Table 1).

The time series at the Summit AWS is valuable to validate the MOD10A1 trend for regions of the ice sheet where surface melting is not observed by passive microwave remote sensing and if occurring in contemporary climate, remains rare. At Summit, the declining albedo trends magnitudes among GC-Net and MOD10A1 results for individual months May–July are consistently negative (Table 1).

Coherent interannual variability is evident in the correlation between synchronous GC-Net and MOD10A1 data, as characterized by correlation coefficients above 0.7 in 16 of 25 (or 64 %) cases (Table 1), suggesting that both independent observations capture the same interannual variability.

4.3 Regional albedo trends

Regionally, the albedo decline in recent years is greatest in the ablation area (Fig. 6a). Large scale albedo decline is evident where relatively gradual surface slopes permit wide ablation areas, namely the southwest, northwest and northeast regions. A decreasing duration of snow cover over low albedo glacier ice and an expansion of the bare ice area is observed especially over the southwestern ice sheet ablation area (Tedesco et al., 2011; van As et al., 2011). For 66 % of the ice sheet area, the 12-yr albedo change exceeds the absolute albedo RMSE of 0.041. Averaged over the accumulation area, the albedo decrease (-0.051) exceeds the absolute uncertainty. In the $6.2 \times 10^5 \text{ km}^2$ area above 2500 m where surface melting has not been detected by passive microwave melt retrievals, an albedo decrease (-0.040) is also evident, from 0.842 in year 2000 to 0.803 in 2011 (time correlation = -0.915 , $1 - p > 0.999$), suggesting that the albedo decline is not only driven by active melting but by enhanced grain metamorphism.

The 2000–2011 $S \downarrow$ change is marked by an increase over the northwestern ice sheet and to a lesser extent over the southwestern ice sheet (Fig. 6b). A decreasing $S \downarrow$ trend is evident over the eastern ice sheet.

The 12-yr change in June–August (JJA) $S \downarrow$ and albedo (Fig. 6a,b) is associated with an increase in solar absorption over the ablation area by $45 \times 10^{18} \text{ J}$ (or 45 Exajoules). Using passive microwave melt days to partition this energy using melt duration, the linear regression change indicates an additional 24 EJ is sunk into melting in 2011 compared with 2000, equivalent with a 72 Gt increase in melt water production over the period. According to total energy budget closure simulated by MAR, increased absorbed solar radiation accounts for 85 % of this melt increase from 331 Gt in 2000 to 416 Gt in 2011. Also according to MAR, June–August is when 93 % of the total annual melting occurs. From this, it is possible to conclude that positive feedback prevailing over the ablation area accounts for 81 % of the increase in melt rates. Before examining the albedo feedback amplification of melt further, implications of the radiation budget changes and causal factors are presented.

Greenland ice sheet albedo feedback

J. E. Box et al.

Title Page

Abstract

Introduction

Conclusions

References

Tables

Figures

◀

▶

◀

▶

Back

Close

Full Screen / Esc

Printer-friendly Version

Interactive Discussion



Greenland ice sheet albedo feedback

J. E. Box et al.

Title Page

Abstract

Introduction

Conclusions

References

Tables

Figures

◀

▶

◀

▶

Back

Close

Full Screen / Esc

Printer-friendly Version

Interactive Discussion



In the accumulation area, despite higher overall albedo than the ablation area, the 4.3 times larger area and higher $S \downarrow$ resulted in it absorbing three times more solar energy. Yet, because accumulation area melting is ~ 8 times less in time duration according to passive microwave, most of this additional absorbed solar energy is used not in melting but in snowpack heating. In the likely example, the additional 148 EJ solar energy is sufficient to completely erode the “cold content” of the $1.494 \times 10^6 \text{ km}^2$ accumulation area to a depth of 14 cm, assuming its temperature, density, and specific heat to be -10°C , 360 kg m^{-3} , and $2110 \text{ J kg}^{-1} \text{ K}^{-1}$, respectively. MAR simulates an annual average T_{air} of -24°C and JJA average accumulation area surface skin temperature (T_s) is -10°C . The subsurface temperature should be between these two temperatures. GC-Net observations confirm that the average temperature of the top snow layer is somewhat lower than -10°C in the accumulation area during summer.

4.4 Important role of NAO in 2000–2011 surface climate trends

During summers 2007–2011, the JJA NAO index (data from <http://www.cpc.ncep.noaa.gov/products/precip/CWlink/pna/new.nao.shtml>) has exhibited a persistent negative pattern, with anomalously high sea level pressure centered over Greenland. The 2011 summer average NAO index anomaly was 2.4σ below the 1970–1999 average (Fig. 7).

Consequently, the 2011 atmospheric flow was characterized by warm air advection from the south along the western ice sheet (Fig. 8). The persistence of this pattern 2007–2011 is without precedent in the period of record since 1950. The 2011 Arctic Report Card executive summary indicates a “shift in the Arctic Ocean system since 2006” (<http://www.arctic.noaa.gov/reportcard/exec.summary.html>). The circulation anomaly led to more anticyclonic circulation, with less summer snowfall and larger $S \downarrow$ than normal over the southern portion of the ice sheet, allowing albedo to remain low during the peak $S \downarrow$ period of the summer. Under this circulation regime numerous ice sheet melting records were set (Fettweis et al., 2011c).

Greenland ice sheet albedo feedback

J. E. Box et al.

Title Page

Abstract

Introduction

Conclusions

References

Tables

Figures

◀

▶

◀

▶

Back

Close

Full Screen / Esc

Printer-friendly Version

Interactive Discussion



The MAR simulations reveal a set of inter-related and statistically significant ice sheet surface climate trends in the 2000–2011 period occurring in response to the persistent anomalous circulation (Fig. 8). Over both the ablation and accumulation areas, $S \downarrow$, T_{air} , S_{net} , R_{net} (“Net Radiation”, the sum of S_{net} and L_{net}) and thus melting increased significantly in response to significant decreases in snowfall and albedo (Table 2). The $S \downarrow$ increase is consistent with the $L \downarrow$ decrease given their highly significant ($1 - p = 0.999$) inverse correlation (-0.845). The sum of $L \downarrow$ and $S \downarrow$, (R_{net}) increased. Q_{SH} increased while less negative Q_{LH} indicates less evaporative heat sink. The ratio: rain/snow increased over the ablation area, though not larger than 1σ of the regression residuals.

The signal of increased snowfall with increasing T_{air} over the accumulation area (Fig. 9a) is related to climatic warming enhancement of ocean evaporation and moisture carrying capacity of the air, leading to higher moisture transport inland over the ice sheet and, consequently, higher precipitation (Fettweis et al., 2011b). The relative dominance of cyclonic or anticyclonic conditions impacts the precipitation amount independently of temperature. Over the ablation area there is a negative correlation between snowfall and T_{air} because MAR correctly simulates precipitation falling as rain instead of snow in warm summers. Similar to the positive T_{air} correlation with snowfall (Fig. 9a), warm years are associated with more rainfall over the ice sheet. Rainfall is confirmed to occur on the ice sheet. Using a Nipher shielded gauge, J. Box measured 5 cm rainfall in a single 24 h period in June 1998 at Swiss Camp located at 1150 m along the western slope of the ice sheet. The signal of increased rainfall with increasing T_{air} is expected because as air warms, the fraction of precipitation falling as rain will increase (Fig. 9b). MAR simulations reveal the important role of summer snowfall on increasing surface albedo over the ablation area (Fig. 10a). Note positive correlation dominating in the ablation area. Thus, especially in 2009–2011 summers, modulated by persistent negative NAO index (inducing dominance of anticyclonic conditions), the albedo feedback could be maximized.

4.5 Ice sheet albedo feedback

Over of the ablation area, the 2000–2011 albedo anomalies correlate inversely with the T_{air} anomalies (Fig. 10b), validating the hypothesis that in warmer years, the ice sheet albedo is lower. In contrast, a positive correlation is evident over much of the higher elevation accumulation area, suggesting that during warm years, the albedo *increases*. This is consistent with the positive correlation signal between T_{air} and snowfall (Fig. 9a).

Albedo sensitivity to surface air temperature (α^*), here specified in $\% \text{K}^{-1}$ units is quantified from the linear regression slope between temporally-detrended MODIS MOD10A1 albedo and MAR T_{air} . Negative α^* is concentrated over the ablation area. The strongest negative α^* (albedo darkening sensitivity to T_{air}), between $-11 \% \text{K}^{-1}$ and $-15 \% \text{K}^{-1}$, is found along the southwestern ablation area (Fig. 11a), immediately below the equilibrium line altitude observed to be $\sim 1450 \text{ m}$ (van de Wal et al., 2005) where the seasonal snow cover, once ablated reveals a darker underlying bare and often impurity-rich (Wientjes and Oerlemans, 2010) solid ice surface. Consistent with findings for the terrestrial environment (Qu and Hall, 2007), the strength of albedo feedback is determined more by the surface albedo decrease associated with a loss of seasonal snow cover than the reduction in snow albedo due to snow metamorphosis, because of the large difference between snow and bare ice albedo values.

The opposite pattern; positive α^* is concentrated over the accumulation area. Positive α^* is evident over 46 % of the accumulation area (pink or red areas in Fig. 11a) (See also Fig. 10 pink and red areas), indicating that the accumulation area gains in brightness in warmer years. Again, the positive albedo correlation with T_{air} is consistent with a MAR-simulated increased snowfall in anomalously warm summers (Fig. 9a).

In the lowest $\sim 600 \text{ m}$ elevation of the southwestern ablation area, α^* is less because the glacier ice surface is already somewhat exposed at melt onset because snow cover is thin ($< 0.3 \text{ m}$) (van den Broeke et al., 2008). Further, for an unknown reason, unlike the mid to upper ablation area, impurities concentrate *below* the surface in the lower ablation area (Wientjes and Oerlemans, 2010). Consequently, the lowest

Greenland ice sheet albedo feedback

J. E. Box et al.

Title Page

Abstract

Introduction

Conclusions

References

Tables

Figures

◀

▶

◀

▶

Back

Close

Full Screen / Esc

Printer-friendly Version

Interactive Discussion



1/4 of the ablation area does not produce as large an albedo change from pre-melt to mid-summer when snow cover is completely ablated.

The ice sheet albedo feedback with T_{air} and $S \downarrow$ is positive over the ice sheet ablation area June–August (Fig. 11b). Peak values of above $+45 \text{ W m}^{-2} \text{ K}^{-1}$ occur in the darkest parts of the ablation area, where surface concentration of impurities is greatest and the ablation of winter snow results in a maximum albedo change. Averaged regionally, the southwestern ice sheet has median albedo feedback values peaking at $+25 \text{ W m}^{-2} \text{ K}^{-1}$ at an elevation of 1250 m. Averaged over the ice sheet, the transition from positive to negative albedo feedback occurs at an elevation of 1500 m. Positive (negative) feedback is not confined exclusively to the (accumulation) ablation area, respectively. Rather, the regimes overlap in elevation (Fig. 12).

5 Conclusions

5.1 MAR accuracy

The observationally-constrained MAR simulations compare favorably with surface observations from AWS with RMSE values for downward solar irradiance of 5 % and 1°C for surface air temperature, respectively. High correlation with the AWS data at monthly time scale justified applying regression based calibrations to improve the absolute accuracy of the MAR data.

5.2 MAR climate insights

After a small calibration based on GC-Net AWS data, summer average T_{air} over the ablation and accumulation areas increased significantly, by 0.5°C . Meanwhile, $S \downarrow$ also increased significantly over the much of the ice sheet. The rain to snowfall ratio increased over the ablation area.

Greenland ice sheet albedo feedback

J. E. Box et al.

Title Page

Abstract

Introduction

Conclusions

References

Tables

Figures

◀

▶

◀

▶

Back

Close

Full Screen / Esc

Printer-friendly Version

Interactive Discussion



5.3 Albedo data validation

According to a cross validation with independent GC-Net AWS data, degrading MODIS instrument sensitivity identified by Wang et al. (2012) is not here detected in the MOD10A1 product.

5 Analysis of the AWS data reveal declining albedo trends in the 2000–2010 period to be widespread in individual months from May–September. In 41 of 43 (95 %) of monthly cases May–September, a decreasing trend is found to exceed 2σ of the regression residuals. In 10 of 14 (71 %) cases for which both GC-Net and MOD10A1 trends are significant, the GC-Net trend declining trend is even larger than the MOD10A1 trend.

10 The coherent interannual variability evident in the correlation between synchronous GC-Net and MOD10A1 data, suggests that at monthly time scales both observations capture the same climate variability.

We have ruled out that degradation of the GC-Net photoelectric diode pyranometers are producing an erroneous declining albedo trend.

15 At the GC-Net Summit AWS where surface melting is not detected by passive microwave remote sensing, the declining albedo trends magnitudes among GC-Net and MOD10A1 results for individual months May–July are consistently negative.

20 Consistent with the MOD10A1 result, the largest magnitude declining albedo trends are evident at the sites located in the ablation zone such as JAR1 and Swiss Camp. Similarly consistent among these independent albedo change results, the more southerly yet relatively high elevation sites of Saddle and South Dome where melting is not common in passive microwave observations, declining albedo trends are observed consistently in individual months.

5.4 Albedo decline and feedbacks

25 MODIS MOD10A1 albedo data indicate a significant ice sheet albedo decline (-0.056 ± 0.007) in the June–August period over the 12 melt seasons spanning 2000–2011. The albedo decline is the largest in magnitude over the ablation area

TCD

6, 593–634, 2012

Greenland ice sheet albedo feedback

J. E. Box et al.

Title Page

Abstract

Introduction

Conclusions

References

Tables

Figures

◀

▶

◀

▶

Back

Close

Full Screen / Esc

Printer-friendly Version

Interactive Discussion



(-0.091 ± 0.021 on average) where bare ice area is increasingly exposed and earlier in the melt period after winter seasonal snow cover ablates reveals a darker glacier ice surface with abundant impurities. A significant albedo decline of 0.046 ± 0.006 in the 2000–2011 period from a year 2000 value of 0.830 is observed for the accumulation area, where warming surface temperatures are enhancing snow grain metamorphosis.

Reduced summer snowfall rates sustained low albedo, maximizing surface solar heating, progressively lowering albedo over multiple years. The albedo declines exceed the absolute RMSE found to be 0.041 using AWS data on the monthly time scale.

Year 2011 albedo over the Greenland ice sheet is the lowest observed in the 12 years since MODIS observations began (day 65 year 2000). As in year 2010, 2011 albedos are more than 1σ below the 2000–2011 average.

The accumulation area albedo decline is attributable to decreases in summer snowfall and winter accumulation and atmospheric sensible heat import promoted by a persistent negative NAO index.

The snow surface albedo feedback for the ice sheet is positive over the ablation area and negative over much of the accumulation area.

Over the ablation area, the albedo sensitivity to surface air temperature reaches peak values of $-12\% \text{ K}^{-1}$ range over the southwestern ice sheet ablation area at an elevation of ~ 1350 m, just below equilibrium line altitude. Detrended albedo anomalies correlate significantly with snowfall rates. Higher albedo is associated with higher summer snowfall rates. Snowfall rates correlate with surface air temperature (correlation = 0.509, $1 - p = 0.909$). Downward solar irradiance combined with albedo sensitivity data provide a quantitative assessment of the albedo feedback. Summer averaged positive albedo feedback values peak magnitude exceeds $+25 \text{ W m}^{-2} \text{ K}^{-1}$ over the ablation area where in years 2010 and 2011, more than half of the increased ablation (93 ± 42 mm over the ablation area) is attributable to albedo feedback.

The negative albedo feedback dominated upper accumulation area, a.k.a. the “dry snow zone” exhibits statistically robust values of $-7 \text{ W m}^{-2} \text{ K}^{-1}$. The negative albedo feedback in this region is promoted by a positive correlation between summer surface

Greenland ice sheet albedo feedback

J. E. Box et al.

Title Page

Abstract

Introduction

Conclusions

References

Tables

Figures

◀

▶

◀

▶

Back

Close

Full Screen / Esc

Printer-friendly Version

Interactive Discussion



Greenland ice sheet albedo feedback

J. E. Box et al.

Title Page

Abstract

Introduction

Conclusions

References

Tables

Figures

◀

▶

◀

▶

Back

Close

Full Screen / Esc

Printer-friendly Version

Interactive Discussion



air temperature and snowfall. The brightening effect of summer precipitation, pronounced in anomalously warm years, is the basis of the negative albedo feedback to limit melting. Thus, accumulation area melting is limited not only because of the normal atmospheric cooling with increasing altitude but that negative albedo feedback limits surface solar heating. As a result of surface brightening resulting from increased snowfall, the accumulation area negative albedo feedback is important in maintaining the ice sheet. The tendency is ironically toward maintaining the ice sheet during climate warming. Competing factors such as a more positive surface radiation balance or sensible heat import by advection may overwhelm the negative albedo feedback's ability to maintain sub-freezing temperatures.

The positive albedo feedback prevailing over the ablation area is responsible for more than half of the increased melt in that region in the last 2 years (2010 and 2011). Without these two extreme years, it would not be clear whether albedo feedback had played an increased role. The key aspect that sets 2010 and 2011 apart from previous years is the combined effect of reduced summer snowfall and sensible heat import from warm air advection triggered by persistent anomalous atmospheric circulation.

5.5 Summer NAO importance

A persistent negative summer NAO index in the 2000's has promoted along Western Greenland a chain reaction of feedbacks. Three key mechanisms emerge that amplify melting: 1.) increased warm (south) air advection along the western ice sheet increases downward sensible heating. In turn, snow metamorphism increases ice grain radii, reducing surface albedo. For areas where the surface is melting, increased liquid water content further reduces the albedo; 2.) clear sky conditions favored by anomalously high surface pressure promotes reduced cloudiness. In turn, diabatic heating by $S \downarrow$ is increased and 3.) reduced summer snowfall precipitation promotes continued snow metamorphosis, keeping the surface in a darkened state and, in low accumulation areas, pre-conditioning the following melt season for enhanced melting. All three

mechanisms work together in a complex feedback revealed by examination of surface energy budget shifts in response to atmospheric circulation.

5.6 Accumulation area radiation budget shift

In the 12 years beginning in 2000, the reduced albedo combined with a significant increase in downward solar irradiance yielded an accumulation area net radiation increase from -0.9 to -0.2 W m^{-2} . Another similar decade may be sufficient to shift the average summer accumulation area radiation budget from negative to positive, resulting in an abrupt ice sheet melt area increase. The ice sheet mass budget deficit is therefore expected to become more sensitive to increasing temperatures via the ice albedo feedback, especially in negative summer NAO index conditions. Future work should therefore be concerned with understanding potential tipping points in ice sheet melt regime as the average radiation budget shifts from negative (cooling) to positive (heating), as it seems the threshold of this has just been reached. It will take some time, perhaps years for the cold content of the firn to be sufficiently eroded to allow continuous summer melting and an ice sheet surface characterized by 100 % melt extent. Further warming would only hasten the amplification of melting that the albedo feedback permits.

Acknowledgements. Research at The Ohio State University was supported by its Climate Water and Carbon initiative managed by D. Alsdorf. D. Decker and R. Benson gathered the MOD10A1 data. N. E. DiGirolamo (SSAI & NASA GSFC) provided data tile stitching insight. K. Steffen supported the transport of the Nipher shielded precipitation gauge to/from Swiss Camp. N. Steiner provided insight into passive microwave melt days retrievals and assisted in citation database management in early versions of this manuscript. This is Byrd Polar Research Center contribution number 1420. Research at the City College of New York was supported by the NASA Cryospheric Program and the NSF grant ARC 0909388. We are very grateful to reviewers for constructive comments.

Greenland ice sheet albedo feedback

J. E. Box et al.

Title Page

Abstract

Introduction

Conclusions

References

Tables

Figures

◀

▶

◀

▶

Back

Close

Full Screen / Esc

Printer-friendly Version

Interactive Discussion



References

- Abdalati, W. and Steffen, K.: Greenland ice sheet melt extent: 1979–1999, *J. Geophys. Res.-Atmos.*, 106(D24), 33983–33988, doi:10.1029/2001jd900181, 2001. 596, 602
- van As, D., Hubbard, A., Hasholt, B., Mikkelsen, A. B., van den Broeke, M., and Fausto, R. S.: Surface mass budget and meltwater discharge from the Kangerlussuaq sector of the Greenland ice sheet during record-warm year 2010, *The Cryosphere Discuss.*, 5, 2319–2347, doi:10.5194/tcd-5-2319-2011, 2011. 607
- Bamber, J. L., Layberry, R. L. and Gogineni, S.: A new ice thickness and bed data set for the Greenland ice sheet 1. Measurement, data reduction, and errors, *J. Geophys. Res.-Atmos.*, 106(D24), 33773–33780, doi:10.1029/2001jd900054, 2001. 600
- Bøggild, C. E., Brandt, R. E., Brown, K. J., Warren, S. G.: The ablation zone in Northeast Greenland: ice types, albedos and impurities, *J. Glaciol.*, 56, 101–113, 2010. 604
- Box, J. E., Bromwich, D. H., Veenhuis, B. A., Bai, L.-S., Stroeve, J. C., Rogers, J. C., and Wang, S.-H.: Greenland ice sheet surface mass balance variability (1988–2004) from calibrated polar MM5 output, *J. Climate*, 19(12), 2783–2800, doi:10.1175/jcli3738.1, 2006. 595, 596
- van den Broeke, M., van As, D., Reijmer, C., and van de Wal, R.: Assessing and improving the quality of unattended radiation observations in Antarctica, *J. Atmos. Ocean. Tech.*, 21(9), 1417–1431, doi:10.1175/1520-0426(2004)021<1417:aaitqo>2.0.co;2, 2004. 599
- van den Broeke, M., Smeets, P., Ettema, J., van der Veen, C., van de Wal, R., and Oerlemans, J.: Partitioning of melt energy and meltwater fluxes in the ablation zone of the west Greenland ice sheet, *The Cryosphere*, 2, 179–189, doi:10.5194/tc-2-179-2008, 2008. 595, 603, 610
- van den Broeke, M., Bamber, J., Ettema, J., Rignot, E., Schrama, E., van de Berg, W. J., and Wouters, B.: Partitioning recent Greenland mass loss, *Science*, 326(5955), 984–986, doi:10.1126/science.1178176, 2009. 595
- van den Broeke, M. R., Smeets, C. J. P. P., and van de Wal, R. S. W.: The seasonal cycle and interannual variability of surface energy balance and melt in the ablation zone of the west Greenland ice sheet, *The Cryosphere*, 5, 377–390, doi:10.5194/tc-5-377-2011, 2011. 604
- Chang, A. T. C., Gloersen, P., Schumge, T., Wilheit, T. T., and Zwally, H. J.: Microwave emission from snow and glacier ice, *J. Glaciol.*, 16(74), 23–39, 1976. 602
- Chen, J. L., Wilson, C. R., and Tapley, B. D.: Interannual variability of Greenland ice losses from

TCD

6, 593–634, 2012

Greenland ice sheet albedo feedback

J. E. Box et al.

Title Page

Abstract

Introduction

Conclusions

References

Tables

Figures

◀

▶

◀

▶

Back

Close

Full Screen / Esc

Printer-friendly Version

Interactive Discussion



satellite gravimetry, *J. Geophys. Res.-Sol. Ea.*, 116, B07406, doi:10.1029/2010jb007789, 2011. 595

Cuffey, K. M. and Paterson, W.: *The physics of glaciers*, Elsevier, pp. 693, 2010. 604

Dee, D. P., Uppala, S. M., Simmons, A. J., Berrisford, P., Poli, P., Kobayashi, S., Andrae, U.,
5 Balmaseda, M. A., Balsamo, G., Bauer, P., Bechtold, P., Beljaars, A. C. M., van de Berg,
L., Bidlot, J., Bormann, N., Delsol, C., Dragani, R., Fuentes, M., Geer, A. J., Haimberger,
L., Healy, S. B., Hersbach, H., Hólm, E. V., Isaksen, L., Kållberg, P., Köhler, M., Matricardi,
M., McNally, A. P., Monge-Sanz, B. M., Morcrette, J.-J., Park, B.-K., Peubey, C., de Ros-
10 nay, P., Tavolato, C., Thépaut, J.-N., Vitart, F.: The ERA-Interim reanalysis: configuration
and performance of the data assimilation system, *Q. J. Roy. Meteor. Soc.*, 137, 553–597,
doi:10.1002/qj.828, 2011. 600

Dozier, J., Schneider, S. R., and McGinnis, D. F.: Effect of grain-size and snowpack water
equivalence on visible and near-infrared satellite-observations of snow, *Water Resour. Res.*,
17(4), 1213–1221, doi:10.1029/WR017i004p01213, 1981. 595

15 Ettema, J., van den Broeke, M. R., van Meijgaard, E., van de Berg, W. J., Bamber, J. L.,
Box, J. E., and Bales, R. C.: Higher surface mass balance of the Greenland ice
sheet revealed by high-resolution climate modeling, *Geophys. Res. Lett.*, 36, L12501,
doi:10.1029/2009gl038110, 2009. 595

Fernandes, R., Zhao, H., Wang, X., Key, J., Qu, X., and Hall, A.: Controls on Northern Hemi-
20 sphere snow albedo feedback quantified using satellite Earth observations, *Geophys. Res.
Lett.*, 36, L21702, doi:10.1029/2009gl040057, 2009. 595

Fettweis, X.: Reconstruction of the 1979–2006 Greenland ice sheet surface mass balance
using the regional climate model MAR, *The Cryosphere*, 1, 21–40, doi:10.5194/tc-1-21-2007,
2007. 600

25 Fettweis, X., Gallée, H., Lefebvre, F., and van Ypersele, J. P.: Greenland surface mass balance
simulated by a regional climate model and comparison with satellite-derived data in 1990–
1991, *Clim. Dynam.*, 24(6), 623–640, doi:10.1007/s00382-005-0010-y, 2005. 600

Fettweis, X., Tedesco, M., van den Broeke, M., and Ettema, J.: Melting trends over the Green-
land ice sheet (1958–2009) from spaceborne microwave data and regional climate models,
30 *The Cryosphere*, 5, 359–375, doi:10.5194/tc-5-359-2011, 2011a. 595, 600, 601, 602, 603

Fettweis, X., Belleflamme, A., Ericum, M., Franco, B., and Nicolay, S.: Estimation of the sea
level rise by 2100 resulting from changes in the surface mass balance of the Greenland ice
sheet, in: *Climate Change – Geophysical Foundations and Ecological Effects*, edited by:

TCD

6, 593–634, 2012

Greenland ice sheet albedo feedback

J. E. Box et al.

Title Page

Abstract

Introduction

Conclusions

References

Tables

Figures

◀

▶

◀

▶

Back

Close

Full Screen / Esc

Printer-friendly Version

Interactive Discussion



Greenland ice sheet albedo feedback

J. E. Box et al.

Title Page

Abstract

Introduction

Conclusions

References

Tables

Figures

◀

▶

◀

▶

Back

Close

Full Screen / Esc

Printer-friendly Version

Interactive Discussion



Blanco, J. and Kheradmand, H., ISBN 978-953-307-419-1, Hard cover, 520 pp., 2011b. 600, 609

Fettweis, X., Mabilille, G., Ericum, M., Nicolay, S., and van den Broeke, M.: The 1958–2009 Greenland ice sheet surface melt and the mid-tropospheric atmospheric circulation, *Clim. Dynam.*, 36(1–2), 139–159, doi:10.1007/s00382-010-0772-8, 2011c. 608

Flanner, M. G., Shell, K. M., Barlage, M., Perovich, D. K., and Tschudi, M. A.: Radiative forcing and albedo feedback from the Northern Hemisphere cryosphere between 1979 and 2008, *Nat. Geosci.*, 4(3), 151–155, doi:10.1038/ngeo1062, 2011. 595

Gallée, H. and Schayes, G.: Development of a three-dimensional meso-gamma primitive equation model: katabatic winds simulation in the area of Terra Nova Bay, Antarctica, *Mon. Weather Rev.*, 122(4), 671–685, doi:10.1175/1520-0493(1994)122<0671:doatdm>2.0.co;2, 1994. 600

Hall, A.: The role of surface albedo feedback in climate, *J. Climate*, 17(7), 1550–1568, doi:10.1175/1520-0442(2004)017<1550:trosaf>2.0.co;2, 2004. 595

Hall, D. K., Williams, Jr., R. S., Luthcke, S. B., and Digirolamo, N. E.: Greenland ice sheet surface temperature, melt and mass loss: 2000–2006, *J. Glaciol.*, 54(184), 81–93, doi:10.3189/002214308784409170, 2008. 597

Hall, D. K., Riggs, G. A., and Salomonson, V. V.: MODIS/Terra Snow Cover Daily L3 Global 500 m Grid V004, January to March 2003, Digital media, updated daily. National Snow and Ice Data Center, Boulder, CO, USA, 2011. 597

Howat, I. M., Smith, B. E., Joughin, I., and Scambos, T. A.: Rates of Southeast Greenland ice volume loss from combined ICESat and ASTER observations, *Geophys. Res. Lett.*, 35(17), L17505, doi:10.1029/2008gl034496, 2008. 595

Klein, A. G. and Barnett, A. C.: Validation of daily MODIS snow cover maps of the Upper Rio Grande River Basin for the 2000–2001 snow year, *Remote Sens. Environ.*, 86(2), 162–176, doi:10.1016/s0034-4257(03)00097-x, 2003. 597

Klein, A. G. and Stroeve, J. C.: Development and validation of a snow albedo algorithm for the MODIS instrument, edited by: Winther, J. G. S. R., *Ann. Glaciol.*, 34, 45–52, 2002. 597

Knap, W. H. and Oerlemans, J.: The surface albedo of the Greenland ice sheet: satellite-derived and in situ measurements in the Sondre Stromfjord area during the 1991 melt season, *J. Glaciol.*, 42(141), 364–374, 1996. 599, 604

Konzelmann, T. and Ohmura, A.: Radiative fluxes and their impact on the energy-balance of the Greenland ice-sheet, *J. Glaciol.*, 41(139), 490–502, 1995. 598, 604

Greenland ice sheet albedo feedback

J. E. Box et al.

Title Page

Abstract

Introduction

Conclusions

References

Tables

Figures

◀

▶

◀

▶

Back

Close

Full Screen / Esc

Printer-friendly Version

Interactive Discussion



- Krabill, W., Hanna, E., Huybrechts, P., Abdalati, W., Cappelen, J., Csatho, B., and Yungel, J.: Greenland ice sheet: increased coastal thinning, *Geophys. Res. Lett.*, 31(24), L24402, doi:10.1029/2004gl021533, 2004. 595
- 5 Lefebre, F., Gallée, H., van Ypersele, J. P., and Greuell, W.: Modeling of snow and ice melt at ETH Camp (West Greenland): a study of surface albedo, *J. Geophys. Res.-Atmos.*, 108(D8), 4231, doi:10.1029/2001jd001160, 2003. 600
- Lefebre, F., Fettweis, X., Gallée, H., Van Ypersele, J. P., Marbaix, P., Greuell, W., and Calanca, P.: Evaluation of a high-resolution regional climate simulation over Greenland, *Clim. Dynam.*, 25(1), 99–116, doi:10.1007/s00382-005-0005-8, 2005. 600
- 10 Mote, T. L.: Greenland surface melt trends 1973–2007: evidence of a large increase in 2007, *Geophys. Res. Lett.*, 34(22), L22507, doi:10.1029/2007gl031976, 2007. 595, 602, 605, 606
- Mote, T. L. and M. R. Anderson M. R.: Variations in snowpack melt on the Greenland ice sheet based on passive-microwave measurements, *J. Glaciol.*, 41, 51–60, 1995. 602
- Pritchard, H. D., Arthern, R. J., Vaughan, D. G., and Edwards, L. A.: Extensive dynamic thinning on the margins of the Greenland and Antarctic ice sheets, *Nature*, 461(7266), 971–975, doi:10.1038/nature08471, 2009. 595
- 15 Qu, X. and Hall, A.: What controls the strength of snow-albedo feedback?, *J. Climate*, 20(15), 3971–3981, doi:10.1175/jcli4186.1, 2007. 610
- Rignot, E. and Kanagaratnam, P.: Changes in the velocity structure of the Greenland ice sheet, *Science*, 311(5763), 986–990, doi:10.1126/science.1121381, 2006. 595
- 20 Rignot, E., Box, J. E., Burgess, E., and Hanna, E.: Mass balance of the Greenland ice sheet from 1958 to 2007, *Geophys. Res. Lett.*, 35(20), L20502, doi:10.1029/2008gl035417, 2008. 594
- Rignot, E., Velicogna, I., van den Broeke, M. R., Monaghan, A., and Lenaerts, J.: Acceleration of the contribution of the Greenland and Antarctic ice sheets to sea level rise, *Geophys. Res. Lett.*, 38, L05503, doi:10.1029/2011gl046583, 2011.
- 25 Steffen, K., Box, J. E., and Abdalati W.: Greenland climate network: GCNet, US Army Cold Regions Reattach and Engineering (CRREL), CRREL Special Report, 98–103, 1996. 596
- Stroeve, J.: Assessment of Greenland albedo variability from the advanced very high resolution radiometer Polar Pathfinder data set, *J. Geophys. Res.-Atmos.*, 106(D24), 33989–34006, doi:10.1029/2001jd900072, 2001. 595
- 30 Stroeve, J. C., Box, J. E., and Haran, T.: Evaluation of the MODIS (MOD10A1) daily snow albedo product over the Greenland ice sheet, *Remote Sens. Environ.*, 105(2), 155–171,

doi:10.1016/j.rse.2006.06.009, 2006. 596, 598

Tedesco, M.: Snowmelt detection over the Greenland ice sheet from SSM/I brightness temperature daily variations, *Geophys. Res. Lett.*, 34(2), L02504, doi:10.1029/2006gl028466, 2007. 602, 604, 606

5 Tedesco, M., Fettweis, X., van den Broeke, M. R., van de Wal, R. S. W., Smeets, C. J. P. P., van de Berg, W. J., Serreze, M. C., and Box, J. E.: The role of albedo and accumulation in the 2010 melting record in Greenland, *Environ. Res. Lett.*, 6, 014005, doi:10.1088/1748-9326/6/1/014005, 2011. 600, 603, 605, 607

10 van de Wal, R. S. W., Greuell, W., van den Broeke, M. R., Reijmer, C. H., and Oerlemans, J.: Surface mass-balance observations and automatic weather station data along a transect near Kangerlussuaq, West Greenland, edited by: Dowdeswell, J. and Willis, I. C., *Ann. Glaciol.*, 42, 311–316, 2005. 610

15 Wang, D., Morton, D., Masek, J., Wu, A., Nagol, J., Xiong, X., Levy, R., Vermote, E., and Wolfe, R.: Impact of sensor degradation on the MODIS NDVI time series, *Remote Sens. Environ.*, 119, 55–61, doi:10.1016/j.rse.2011.12.001, 2011. 605, 612

Warren, S. G.: Optical-properties of snow, *Rev. Geophys.*, 20(1), 67–89, doi:10.1029/RG020i001p00067, 1982. 595

20 Wientjes, I. G. M. and Oerlemans, J.: An explanation for the dark region in the western melt zone of the Greenland ice sheet, *The Cryosphere*, 4, 261–268, doi:10.5194/tc-4-261-2010, 2010. 599, 604, 610

Wiscombe, W. J. and Warren, S. G.: A Model for the spectral albedo of snow, 1. Pure snow, *J. Atmos. Sci.*, 37(12), 2712–2733, doi:10.1175/1520-0469(1980)037<2712:amftsa>2.0.co;2, 1980. 595

Greenland ice sheet albedo feedback

J. E. Box et al.

Title Page

Abstract

Introduction

Conclusions

References

Tables

Figures

◀

▶

◀

▶

Back

Close

Full Screen / Esc

Printer-friendly Version

Interactive Discussion



Table 1. Comparison of albedo trends in MODIS MOD10A1 and GC-Net observations for statistically significant cases.

Month	GC-Net Site	Albedo Data Source	Albedo Trend, decade ⁻¹	Nbr Years	GC-Net vs. MODIS correlation
May	Summit	GC-NET	-0.026	11	0.649
	Summit	MOD10A1	-0.028	11	
	Tunu-N	MOD10A1	-0.033	11	0.888
	DYE-2	GC-NET	-0.034	9	
	DYE-2	MOD10A1	-0.030	9	0.733
	Saddle	GC-NET	-0.040	11	
	Saddle	MOD10A1	-0.030	11	0.826
	NASA-E	MOD10A1	-0.035	9	
	NASA-SE	MOD10A1	-0.027	8	-0.036
	JAR2	GC-NET	-0.188	8	
Jun	CP1	GC-NET	0.076	7	0.768
	Summit	GC-NET	-0.026	10	
	Summit	MOD10A1	-0.023	10	-0.452
	Tunu-N	GC-NET	0.022	8	
	DYE-2	GC-NET	-0.044	8	0.820
	DYE-2	MOD10A1	-0.040	8	
	JAR1	GC-NET	-0.268	9	0.938
	Saddle	GC-NET	-0.048	8	
	Saddle	MOD10A1	-0.032	8	0.919
	JAR2	GC-NET	-0.089	9	
Jul	Swiss Camp	GC-NET	-0.134	8	0.907
	Swiss Camp	MOD10A1	-0.161	8	
	CP1	MOD10A1	-0.049	8	0.695
	Summit	GC-NET	-0.031	10	
	Summit	MOD10A1	-0.031	10	0.790
	DYE-2	GC-NET	-0.054	7	
	JAR1	GC-NET	-0.343	10	0.948
	Saddle	GC-NET	-0.066	9	
	Saddle	MOD10A1	-0.050	9	0.876
	South Dome	GC-NET	-0.075	7	
South Dome	MOD10A1	-0.041	7	0.772	
NASA-SE	GC-NET	-0.071	7		
NASA-SE	MOD10A1	-0.051	7	0.787	
JAR2	MOD10A1	-0.070	9		
Aug	Swiss Camp	GC-NET	-0.198	7	0.869
	Swiss Camp	MOD10A1	-0.293	7	
	DYE-2	GC-NET	-0.053	7	0.843
	JAR1	GC-NET	-0.239	11	
	JAR1	MOD10A1	-0.288	11	0.693
	JAR2	MOD10A1	-0.097	9	
Sep	Summit	GC-NET	-0.055	8	0.220
	JAR1	GC-NET	-0.369	9	
	JAR1	GC-NET	-0.369	9	0.491
	JAR2	GC-NET	-0.133	9	

**Greenland ice sheet
albedo feedback**

J. E. Box et al.

Title Page

Abstract Introduction

Conclusions References

Tables Figures

◀ ▶

◀ ▶

Back Close

Full Screen / Esc

Printer-friendly Version

Interactive Discussion



Greenland ice sheet
albedo feedback

J. E. Box et al.

Table 2. Ice sheet summer (June–August) surface climate variability 2000–2011 partitioned among ablation and accumulation areas by annual surface mass balance.

Parameter	units	Ablation Area			Accumulation Area		
		Average	Linear Change	St. Dev. Residuals	Average	Linear Change	St. Dev. Residuals
T_{air}	°C	-1.6	0.5	0.4	-8.8	0.5	0.5
Snow	mm w.e.	15.9	-6.9	2.1	28.2	-7.3	3.4
Rain	mm w.e.	39.3	-10.4	10.4	6	-2	1.5
Rain/Snow	none	2.5	0.4	0.7	0.2	0	0
$S \downarrow$	W m^{-2}	280.9	5.4	3.8	296.3	3.4	3
S_{net}	W m^{-2}	110.8	11	7.4	60.5	2.3	1.6
$L \downarrow$	W m^{-2}	242.1	-1.3	3.5	209.4	0.6	4.1
L_{net}	W m^{-2}	-64.6	-2.7	3.1	-61	-1.5	2.1
$S \downarrow + L \downarrow$	W m^{-2}	523	4.2	1.5	505.8	4	1.9
R_{net}	W m^{-2}	46.2	8.3	6.2	-0.5	0.8	0.7
Q_{SH}	W m^{-2}	17.7	3.2	2.1	5	0.1	0.5
Q_{LH}	W m^{-2}	-4.5	0.3	0.8	-0.6	0.1	0.2
$Q_{\text{SH}} + Q_{\text{LH}}$	W m^{-2}	13.1	3.4	1.9	4.4	0.2	0.4
α_{MOD10A1}	none	0.673	-0.091	0.021	0.809	-0.046	0.006
Melt	mm w.e.	1257.9	261.5	158	123.9	18.1	18.2

Title Page

Abstract

Introduction

Conclusions

References

Tables

Figures

I◀

▶I

◀

▶

Back

Close

Full Screen / Esc

Printer-friendly Version

Interactive Discussion



Greenland ice sheet
albedo feedback

J. E. Box et al.

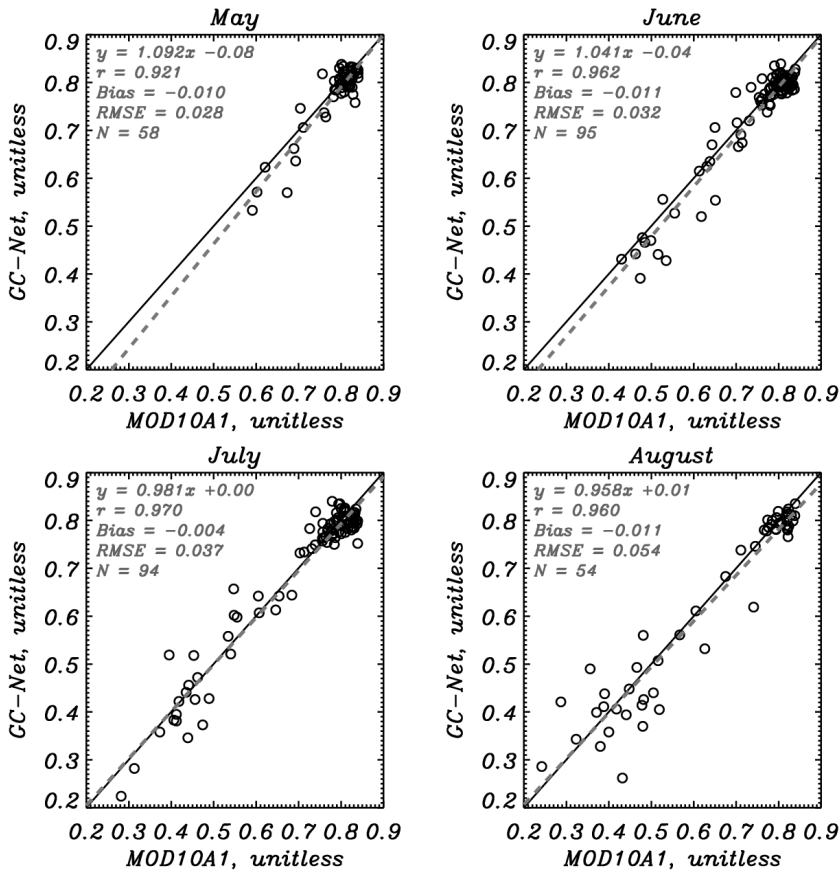


Fig. 1. Comparison of monthly averaged MODIS MOD10A1 albedo values less than 0.84 with observations from 17 GC-Net automatic weather stations. The June–August average RMSE is 0.041.

Greenland ice sheet albedo feedback

J. E. Box et al.

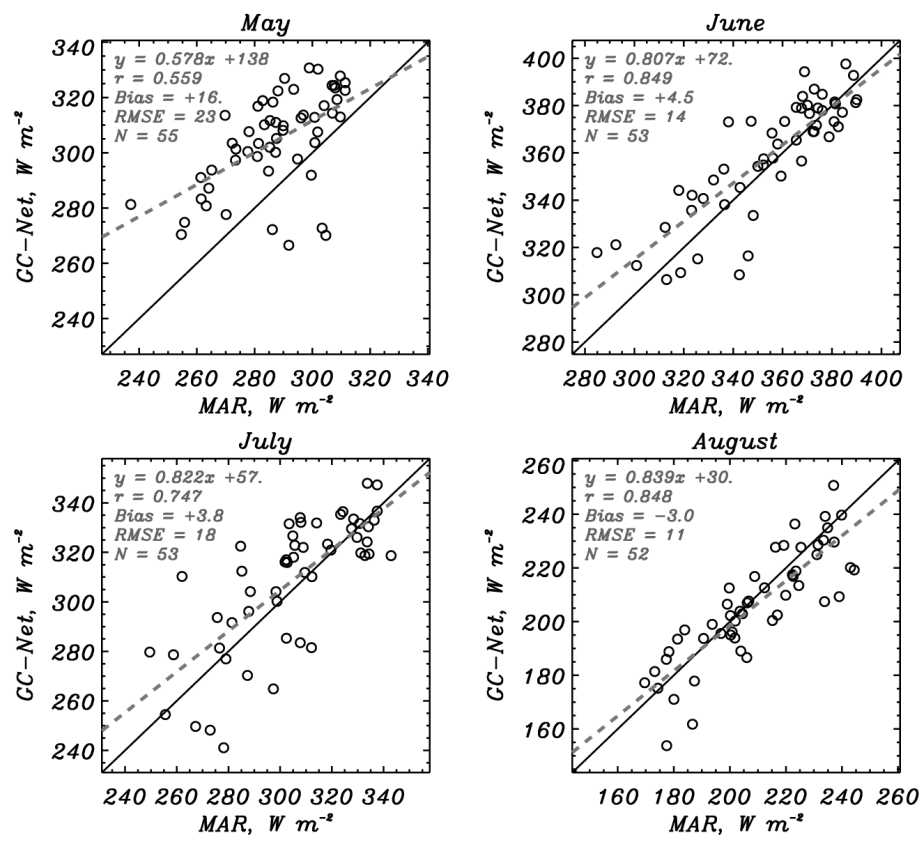


Fig. 2. Comparison of monthly averaged MAR simulations of monthly average downward short-wave irradiance with observations from GC-Net automatic weather stations spanning the 2000–2005 period when GC-Net $S \downarrow$ data are available for this study.

Title Page

Abstract Introduction

Conclusions References

Tables Figures

◀ ▶

◀ ▶

Back Close

Full Screen / Esc

Printer-friendly Version

Interactive Discussion



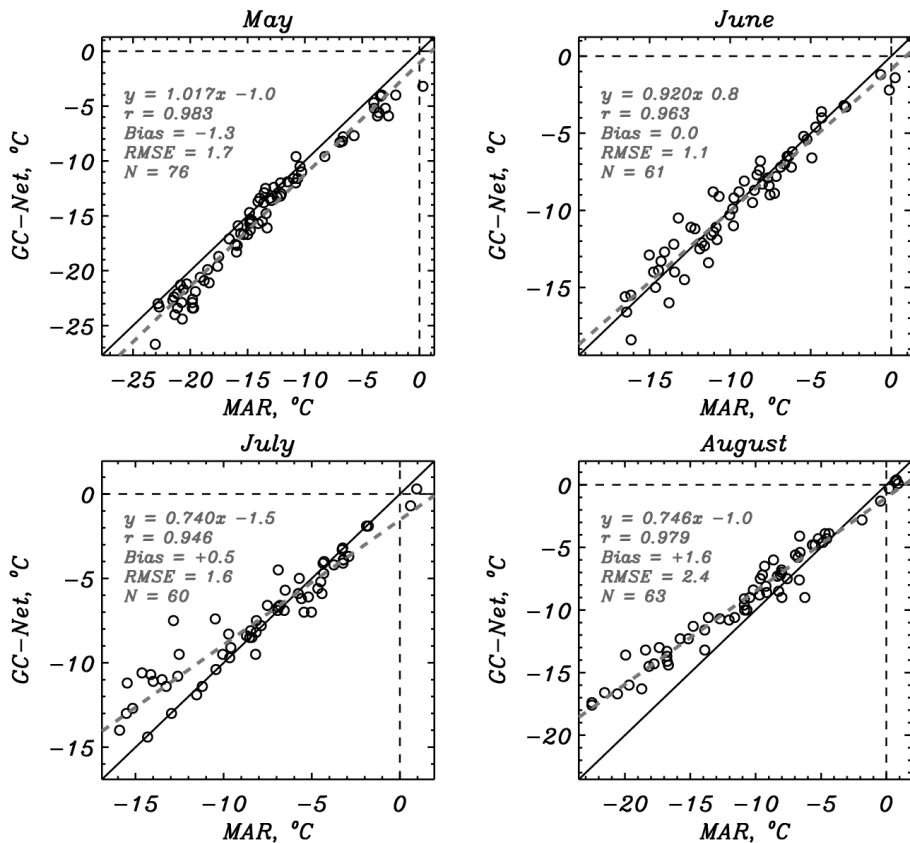


Fig. 3. Comparison of monthly averaged MAR simulations of surface air temperature with observations from GC-Net automatic weather stations for the 2000–2010 when GC-Net T_{air} data are available to this study.

Greenland ice sheet albedo feedback

J. E. Box et al.

Title Page

Abstract Introduction

Conclusions References

Tables Figures

◀ ▶

◀ ▶

Back Close

Full Screen / Esc

Printer-friendly Version

Interactive Discussion



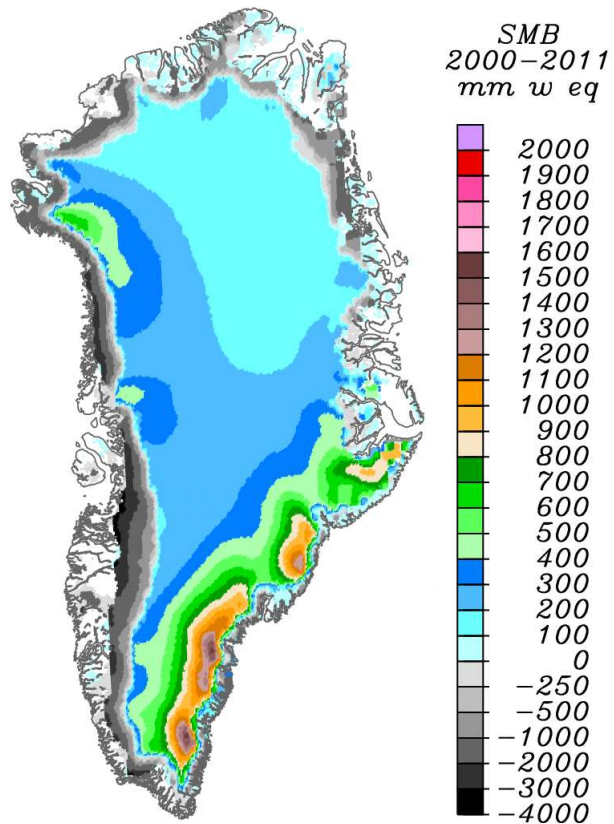


Fig. 4. Surface mass balance averaged spanning the 12 yr of this study (2000–2011) according to MAR simulations. Grey tones indicate the ablation area. Colored regions indicate the accumulation area.

**Greenland ice sheet
albedo feedback**

J. E. Box et al.

Title Page

Abstract Introduction

Conclusions References

Tables Figures

◀ ▶

◀ ▶

Back Close

Full Screen / Esc

Printer-friendly Version

Interactive Discussion



Greenland ice sheet albedo feedback

J. E. Box et al.

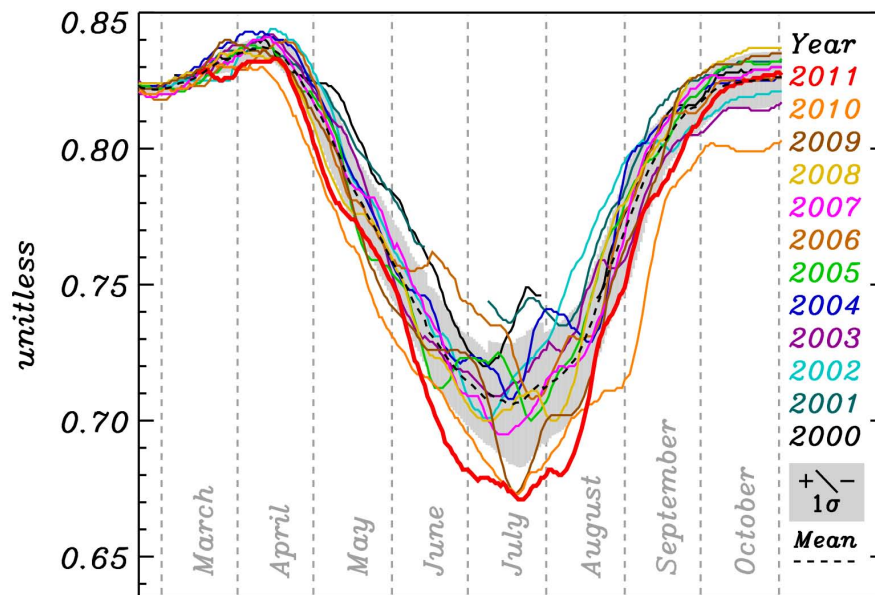


Fig. 5. 11-day running median Greenland ice sheet albedo from Moderate Resolution Imaging Spectroradiometer (MODIS) MOD10A1 data. The dashed line represents the 2000–2011 daily average.

Title Page

Abstract

Introduction

Conclusions

References

Tables

Figures

◀

▶

◀

▶

Back

Close

Full Screen / Esc

Printer-friendly Version

Interactive Discussion



Greenland ice sheet
albedo feedback

J. E. Box et al.

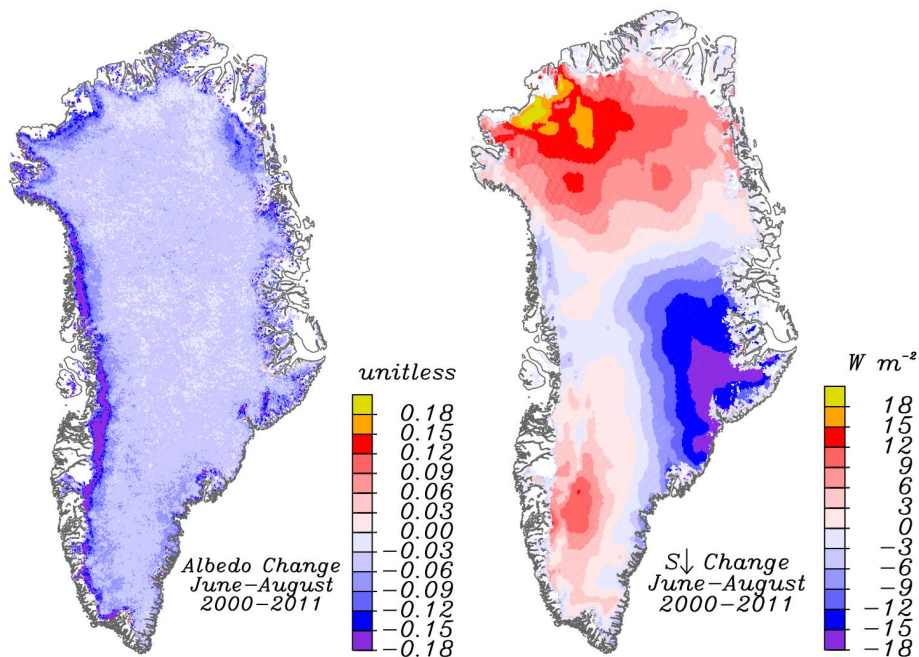


Fig. 6. (a) Summer (June–August) spatial patterns MODIS MOD10A1 5 km albedo temporal change 2000–2011 derived from the linear regression. (b) Summer change in MAR downward shortwave simulations calibrated using GC-Net AWS data.

Discussion Paper | Discussion Paper | Discussion Paper | Discussion Paper | Discussion Paper

Title Page

Abstract

Introduction

Conclusions

References

Tables

Figures

◀

▶

◀

▶

Back

Close

Full Screen / Esc

Printer-friendly Version

Interactive Discussion



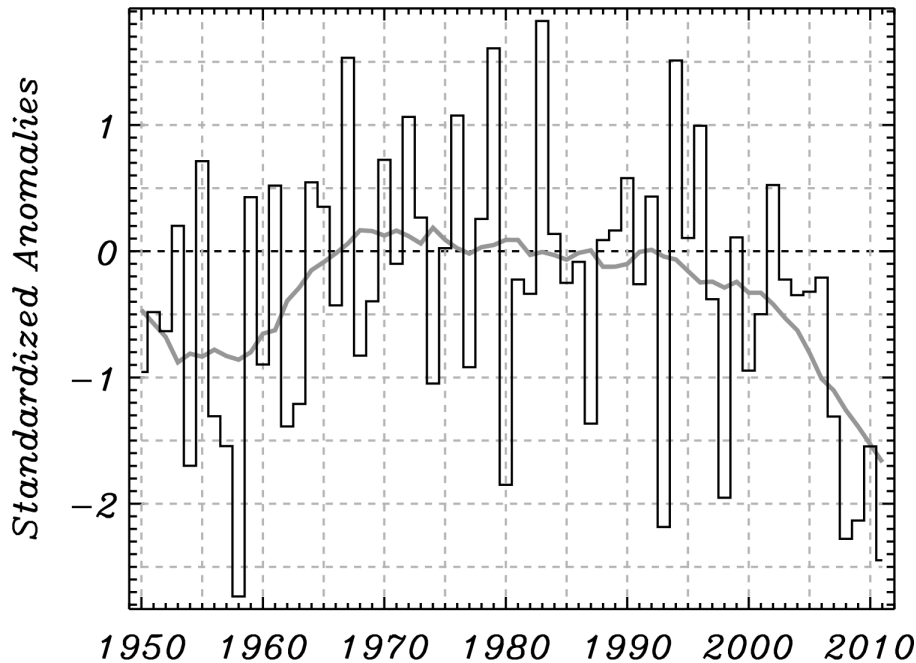


Fig. 7. Summer NAO index anomalies standardized relative to 1970–1999 baseline, indicating an anomalous and persistent negative pattern 2007–2011. The black bars indicate June–August averages of monthly anomalies. The grey line represents an 11-yr 4σ Gaussian running average that becomes increasingly a leading (trailing) average as the beginning (end) point of the time series is reached, respectively.

Greenland ice sheet albedo feedback

J. E. Box et al.

Title Page	
Abstract	Introduction
Conclusions	References
Tables	Figures
◀	▶
◀	▶
Back	Close
Full Screen / Esc	
Printer-friendly Version	
Interactive Discussion	



Greenland ice sheet
albedo feedback

J. E. Box et al.

Title Page

Abstract

Introduction

Conclusions

References

Tables

Figures

◀

▶

◀

▶

Back

Close

Full Screen / Esc

Printer-friendly Version

Interactive Discussion

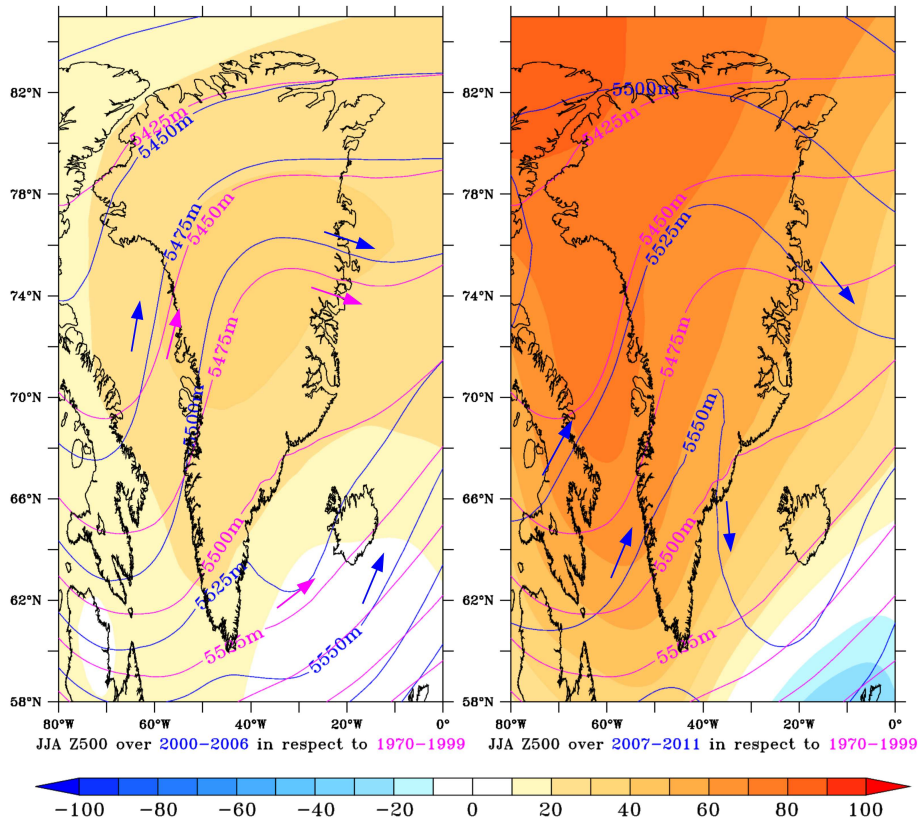


Fig. 8. The geopotential height anomalies for JJA 2000–2006 (a) and 2007–2011 (b) (referenced to the 1970–1999 average) at 500 hPa from the NCEP/NCAR Reanalysis. The blue and respectively magenta lines illustrate the JJA average geopotential height at 500 hPa in 2000–2006 and 2007–2011 and over 1970–1999. The arrows show the direction of the prevailing flow.

Greenland ice sheet
albedo feedback

J. E. Box et al.

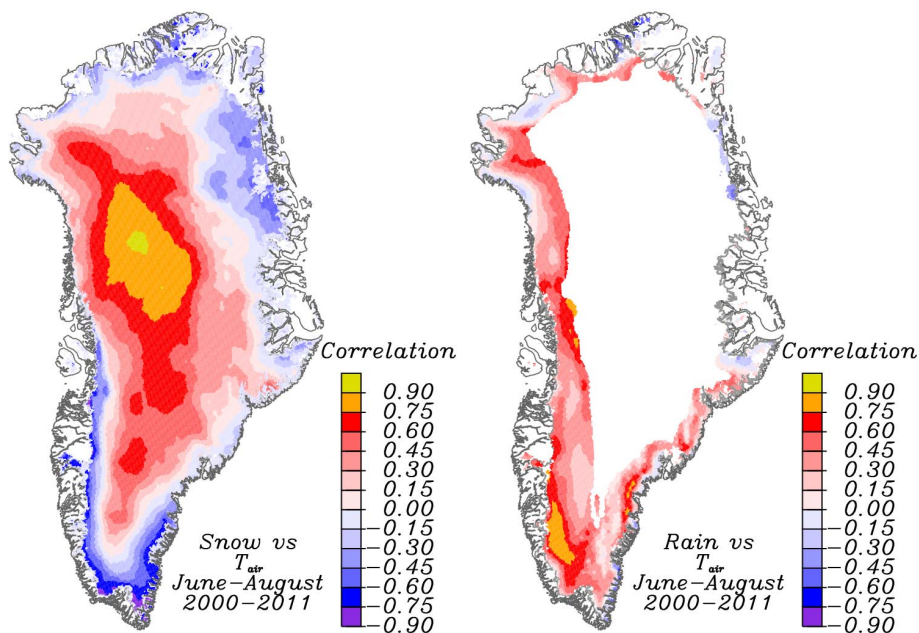


Fig. 9. (a) summer (June–August) spatial patterns of the correlation between 5 km resampled MAR snowfall and 3 m surface air temperature data. (b) same as left but with MAR rainfall instead of snowfall. Values where simulated rainfall is less than 5 mm are excluded because in this limit the values are highly uncertain. The regression variables are first temporally detrended to minimize spurious correlation.

Title Page

Abstract

Introduction

Conclusions

References

Tables

Figures

◀

▶

◀

▶

Back

Close

Full Screen / Esc

Printer-friendly Version

Interactive Discussion



Greenland ice sheet
albedo feedback

J. E. Box et al.

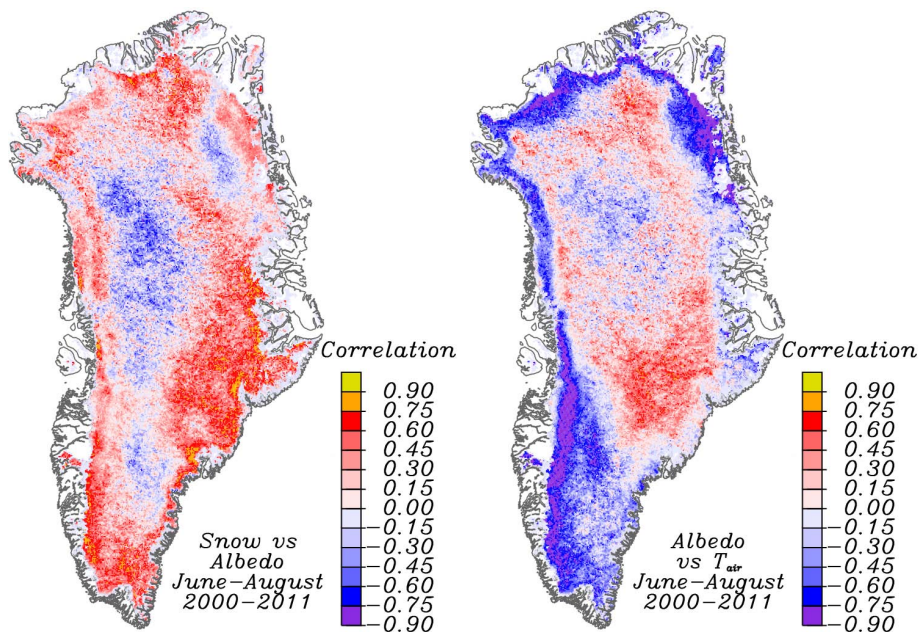


Fig. 10. (a) Summer (June–August) spatial patterns of the correlation between 5 km averaged MODIS MOD10A1 albedo and 25 km averaged MAR snowfall data. (b) Same as the MAR near-surface air temperature data.

Discussion Paper | Discussion Paper | Discussion Paper | Discussion Paper | Discussion Paper

Title Page

Abstract

Introduction

Conclusions

References

Tables

Figures

◀

▶

◀

▶

Back

Close

Full Screen / Esc

Printer-friendly Version

Interactive Discussion



Greenland ice sheet
albedo feedback

J. E. Box et al.

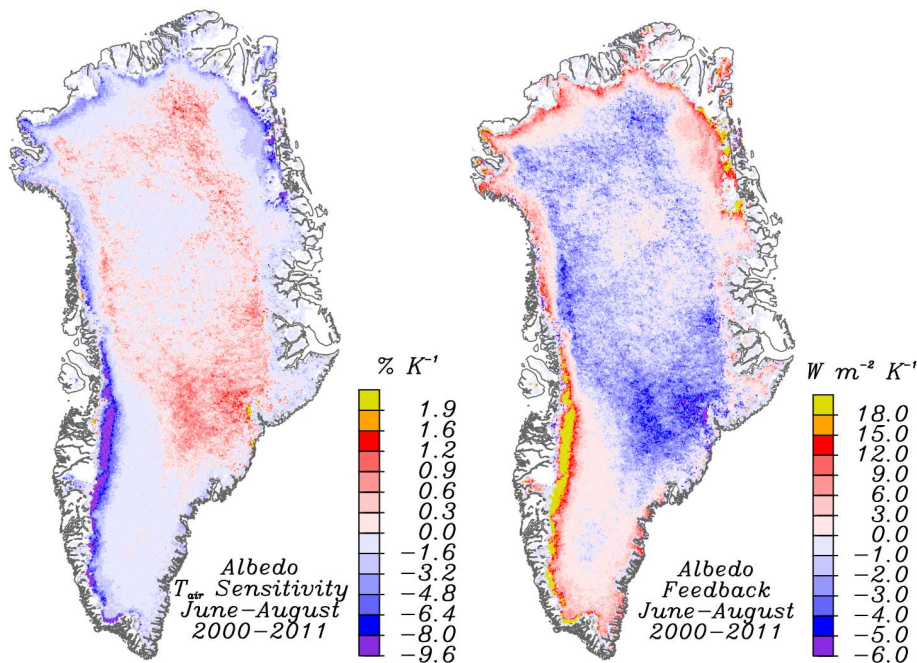


Fig. 11. (a) summer (JJA) spatial patterns of MODIS MOD10A1 albedo sensitivity to the MAR simulated surface air temperature. The positive scale is 1/5th that of the negative scale. (b) summer spatial patterns of ice sheet albedo feedback based on MODIS albedo observations and MAR simulations of S_{\downarrow} , and T_{air} . The negative albedo feedback scale is 1/3rd that of the positive scale. The regressions are detrended to minimize spurious correlation.

Title Page

Abstract

Introduction

Conclusions

References

Tables

Figures

◀

▶

◀

▶

Back

Close

Full Screen / Esc

Printer-friendly Version

Interactive Discussion



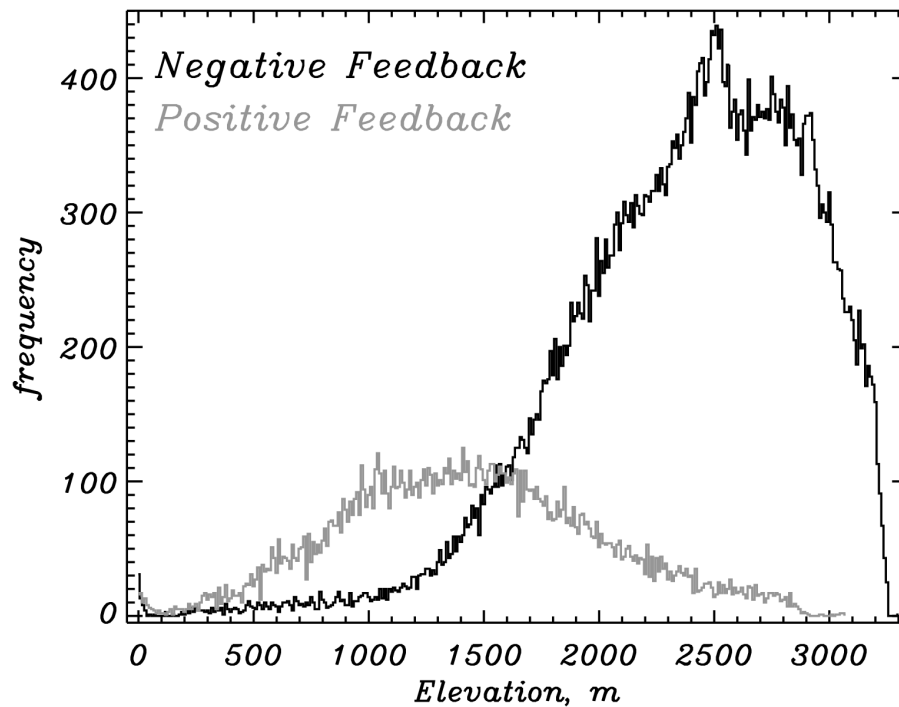


Fig. 12. Elevational histograms of temporally-detrended albedo feedback for the whole ice sheet for 5 km grid cells used in this study

**Greenland ice sheet
albedo feedback**

J. E. Box et al.

Title Page

Abstract Introduction

Conclusions References

Tables Figures

◀ ▶

◀ ▶

Back Close

Full Screen / Esc

Printer-friendly Version

Interactive Discussion

